symmetry

MDPI

Article

Nonlinear Axion Electrodynamics: Axionically Induced Electric Flares in the Early Magnetized Universe

Alexander B. Balakin [1,*], Vladimir V. Bochkarev [2] and Albina F. Nizamieva [1]

[1] Department of General Relativity and Gravitation, Institute of Physics, Kazan Federal University, Kremlevskaya Str. 16a, 420008 Kazan, Russia; alb9061@yandex.ru
[2] Department of Radiophysics, Institute of Physics, Kazan Federal University, Kremlevskaya Str. 16a, 420008 Kazan, Russia; Vladimir.Bochkarev@kpfu.ru
* Correspondence: Alexander.Balakin@kpfu.ru

Abstract: We consider the nonlinearly extended Einstein–Maxwell-axion theory, which is based on the account for two symmetries: first, the discrete symmetry associated with the properties of the axion field, and second, the Jackson's symmetry, prescribing to the electrodynamics to be invariant with respect to the rotation in the plane coordinated by the electric and magnetic fields. We derive the master equations of the nonlinearly extended theory and apply them to the Bianchi-I model with magnetic field. The main result, describing the behavior of the nonlinearly coupled axion, electromagnetic, and gravitational fields is the anomalous growth of the axionically induced electric field in the early magnetized Universe. The character of behavior of this anomalous electric field can be indicated by the term flare. We expect, that these electric flares can produce the electron–positron pair creation, significant acceleration of the born charged particles, and the emission of the electromagnetic waves by these accelerated particles.

Keywords: axion; nonlinear electrodynamics; early Universe

Citation: Balakin, A.B.; Bochkarev, V.V.; Nizamieva, A.F. Nonlinear Axion Electrodynamics: Axionically Induced Electric Flares in the Early Magnetized Universe. *Symmetry* **2021**, *13*, 2038. https://doi.org/10.3390/sym13112038

Academic Editors: Stefano Profumo, Tomohiro Inagaki and Olga Kodolova

Received: 6 October 2021
Accepted: 26 October 2021
Published: 29 October 2021

1. Introduction

The concept of symmetry has played and continues to play an outstanding role in the physics of fundamental interactions. Extending the theoretical models of the nonlinear cosmic axion electrodynamics, we happen to be inspired by beauty of the symmetries of two types. The first type of symmetry is connected with the idea that the Lagrangian of the axion electrodynamics is invariant with respect to the discrete symmetry, associated with the shift $\tilde{\phi} = \phi + 2\pi k$ (k is an integer) of the pseudoscalar field ϕ introduced by Peccei and Quinn [1] and indicated later as an axion field (see, e.g., [2–6] for details of this story). According to this, we need to have a Lagrangian, which contains the invariants based on the Maxwell tensor F_{ik}, its dual F^*_{ik}, and the axion field ϕ introduced nonlinearly. Clearly, the well-known linear term $\phi F^*_{mn} F^{mn}$ supports the discrete symmetry, since the rest term $2\pi k\sqrt{-g}F^*_{mn}F^{mn}$ in the action functional is the perfect divergence and thus can be eliminated. When one deals with the nonlinear modification of the theory, the nonlinear function of the true invariant $f(\phi F^*_{mn}F^{mn})$ does not satisfy the mentioned discrete symmetry, and in this sense, we have to search for new nonlinear terms. For this purpose, we attract for consideration the idea of Jackson [7] that the vacuum Faraday–Maxwell electrodynamics is symmetric with respect to linear transformation of the electric and magnetic fields $\vec{E}_* \to \vec{E}\cos\alpha + \vec{B}\sin\alpha$, $\vec{B}_* \to \vec{B}\cos\alpha - \vec{E}\sin\alpha$, with the constant angle α. Regarding the nonlinear modification of the axion electrodynamics, we assume to use the Lagrangian, which satisfies both mentioned symmetries. The example of such Lagrangian has been constructed in the work [8]. The proposed nonlinear Lagrangian has the form $\mathcal{L}(\mathcal{I})$, where $\mathcal{L}(\mathcal{I})$ is some nonlinear function of its argument, and the invariant $\mathcal{I}$ is

$$\mathcal{I} = \frac{1}{4}(\cos\phi\, F_{mn}F^{mn} + \sin\phi\, F^*_{mn}F^{mn})\,. \tag{1}$$

We assume that for small $\mathcal{I}$ the Lagrangian can be transformed into $\mathcal{L}(\mathcal{I}) \to \mathcal{I}$. In the linear theory, when $\phi \to 0$, the invariant $\mathcal{I}$ can be reduced to the standard invariant

$$\mathcal{I} \to \frac{1}{4}(F_{mn}F^{mn} + \phi F^{*}_{mn}F^{mn}) \tag{2}$$

linear in ϕ and covering the basic term of the linear axion electrodynamics [4,5]. Clearly, the discrete symmetry $\tilde{\phi} = \phi + 2\pi k$ is supported identically by the choice of sin/cosine multipliers in front of the standard terms $F_{mn}F^{mn}$ and $F^{*}_{mn}F^{mn}$. As for the Jackson's symmetry, if we use the transformation

$$\mathcal{F}^{ik} = F^{ik}\cos\frac{\phi}{2} + F^{*ik}\sin\frac{\phi}{2}, \tag{3}$$

we obtain the term $\frac{1}{4}\mathcal{F}^{ik}\mathcal{F}_{ik}$, which coincides with (1). This fact confirms the validity of the symmetry transformations

$$\mathcal{E}^{i} = E^{i}\cos\frac{\phi}{2} + B^{i}\sin\frac{\phi}{2}, \quad \mathcal{B}^{i} = -E^{i}\sin\frac{\phi}{2} + B^{i}\cos\frac{\phi}{2}, \tag{4}$$

which include the electric field four-vector $E^{i} = F^{ik}U_{k}$ and the magnetic induction four-vector $B^{i} = F^{*ik}U_{k}$. The quantity U^{k} is the velocity four-vector of the medium or of an observer.

The nonlinear models with such symmetries attract special attention, since they contain a latent instability which can be displayed by the anomalous growth of the axionically induced electric field. When the model is quasilinear, i.e., when the axion field enters the Lagrangian with sin/cosine nonlinearities but the electromagnetic field is described in the linear context, the problem of electric flares was discussed in the paper [8]. It was shown in [8] that the interaction with the dynamic aether stabilizes the evolution, and the axion field does not reach the catastrophic value $\phi = \frac{\pi}{2}$, which corresponds to the infinite value of the electric field proportional to the $\tan\phi$. Now, we exclude the dynamic aether from the model but consider the electromagnetic field in the nonlinear context. Our goal is to show that in the manifold of the guiding parameters of the model there exists an area, in which the presented model is stable. In particular, this means that the axionically induced electric field is finite, but its amplitude can reach very large values, thus producing the pair creation, particle acceleration, and electromagnetic waves emission in the early magnetized Universe.

The paper is organized as follows: In Section 2, we describe the mathematical formalism of the proposed nonlinear extension of the Einstein–Maxwell-axion theory. In Section 3, we reduce the basic equations taking into account the symmetry of the cosmological anisotropic Bianchi-I model with magnetic field and derive the pair of key equations for the axion field and for the derivative of the scale factor. In Section 4, we analyze the solutions to the key equations using qualitative and numerical methods and discuss the problem of the axionically induced electric field generation. Section 5 contains the discussion and conclusions.

2. Nonlinear Einstein–Maxwell-Axion Model

2.1. The Action Functional and Master Equations of the Model

The model is based on the action functional presented in the form

$$-S = \int d^{4}x\sqrt{-g}\left\{\frac{R+2\Lambda}{2\kappa} + \frac{1}{2}\Psi_{0}^{2}\left[V(\phi) - \nabla_{k}\phi\nabla^{k}\phi\right] + \mathcal{L}(\mathcal{I})\right\}. \tag{5}$$

According to the standards, R is the Ricci scalar, Λ is the cosmological constant, and $\kappa = 8\pi G$ is the Einstein constant (we consider $c = 1$). The dimensionless quantity ϕ describes the pseudoscalar (axion) field, $V(\phi)$ is the potential of the axion field, and ∇_{k} is the covariant derivative. The constant Ψ_{0} is reciprocal to the coupling constant of the

axion–photon interaction $g_{A\gamma\gamma}$, i.e., $\frac{1}{\Psi_0} = g_{A\gamma\gamma} < 1.47 \times 10^{-10}$ GeV^{-1}. Many authors, keeping in mind physical motives, prefer to work with the axion field indicated as a; this quantity can be expressed in terms of ϕ, as follows: $a = \Psi_0\phi$, or equivalently $\phi = g_{A\gamma\gamma} \cdot a$. In this representation, the term $\phi F^*_{mn}F^{mn}$ in (2) converts into $g_{A\gamma\gamma} \cdot aF^*_{mn}F^{mn}$, and the term $\Psi_0^2\nabla_k\phi\nabla^k\phi$ in (5) takes the form of $\nabla_k a\nabla^k a$. The new element of the theory is encoded in the last term $\mathcal{L}(\mathcal{I})$, the Lagrangian of the electromagnetic field interacting with the axion field; this Lagrangian is the nonlinear function of the argument $\mathcal{I}$, which has at least one continuous derivative and tends to $\mathcal{I}$ at $\mathcal{I} \to 0$, i.e., $\mathcal{L}(\mathcal{I} \to 0) \to \mathcal{I}$. The argument $\mathcal{I}$ is presented by (1).

2.1.1. Master Equations for the Electromagnetic Field

The variation of the action functional (5) with respect to the potential of the electromagnetic field A_i yields

$$\nabla_k\Big\{\mathcal{L}'(\mathcal{I})\Big[\cos\phi\, F^{ik} + \sin\phi\, F^{*ik}\Big]\Big\} = 0\,, \tag{6}$$

where the prime denotes the derivative with respect to the argument $\mathcal{I}$. In addition to the nonlinear electrodynamic Equation (6), we use the standard equations

$$\nabla_k F^{*ik} = 0\,, \tag{7}$$

which are the consequence of the definition of the Maxwell tensor $F_{mn} = \nabla_m A_n - \nabla_n A_m$.

As examples, below we consider two model variants of the nonlinear function $\mathcal{L}(\mathcal{I})$. The first one is of the power law type

$$\mathcal{L}(\mathcal{I}) = \mathcal{I} + \gamma\mathcal{I}^\nu\,, \quad \nu > 1\,. \tag{8}$$

The second variant contains the Kohlrausch type function (stretched exponential [9])

$$\mathcal{L}(\mathcal{I}) = \mathcal{I}^{1-\gamma}[\exp(\mathcal{I}^\gamma) - 1]\,, \quad \gamma > 0\,. \tag{9}$$

When $\mathcal{I}$ is small and the parameter γ is positive, the Kohlrausch type function (9) can be linearized as follows: $\mathcal{L}(\mathcal{I}) \to \mathcal{I}^{1-\gamma}\mathcal{I}^\gamma = \mathcal{I}$, thus recovering the model of linear electrodynamics.

2.1.2. Master Equation for the Axion Field

Variation of the action functional (5) with respect to the axion field ϕ gives the equation

$$\nabla^k\nabla_k\phi + \frac{1}{2}\frac{dV(\phi)}{d\phi} = \frac{1}{4\Psi_0^2}\mathcal{L}'(\mathcal{I})\Big[\sin\phi F_{ik}F^{ik} - \cos\phi F_{ik}F^{*ik}\Big]\,. \tag{10}$$

We consider the potential $V(\phi)$ to be of the periodic form

$$V(\phi) = 2m_A^2(1 - \cos\phi)\,. \tag{11}$$

For small values ϕ, the potential (11) converts into the standard one $V(\phi) \to m_A^2\phi^2$, where m_A is the axion mass. Taking into account (11), one can rewrite Equation (10) as follows:

$$\nabla^k\nabla_k\phi = -m_A^2\sin\phi + \frac{1}{4\Psi_0^2}\mathcal{L}'(\mathcal{I})\Big[\sin\phi F_{ik}F^{ik} - \cos\phi F_{ik}F^{*ik}\Big]\,. \tag{12}$$

This equation explicitly satisfies the requirement of the discrete symmetry $\tilde{\phi} = \phi + 2\pi k$.

Remark 1. *Remark about the effective electromagnetic mass of the axion*

For the linear version of electrodynamics and for small values of ϕ, the axion field equation takes the form

$$\nabla^k \nabla_k \phi + m_A^2 \phi = \frac{1}{4\Psi_0^2}\left[\phi F_{ik} F^{ik} - F_{ik} F^{*ik}\right]. \tag{13}$$

Clearly, in the standard axion electrodynamics, the term $\frac{\phi}{4\Psi_0^2} F_{ik} F^{ik}$, proportional to the axion field, did not appear. It is the residual term, which appears due to the sin/cosine extension of the Lagrangian and describes the idea that the axion field can mimic the effects attributed to the dilaton field (see [8] for details). Now, we can rewrite (13) in the following form:

$$\nabla^k \nabla_k \phi + \phi\left(m_A^2 - \frac{1}{4\Psi_0^2} F_{ik} F^{ik}\right) = -\frac{1}{4\Psi_0^2} F_{ik} F^{*ik}. \tag{14}$$

The standard term in the right-hand side of this equation describes the electromagnetic source, which produces the axions. The new term, which contains the quantity

$$M_{(\mathrm{eff})} = \sqrt{m_A^2 - \frac{1}{4\Psi_0^2} F_{ik} F^{ik}}, \tag{15}$$

can be indicated as the effective axion mass $M_{(\mathrm{eff})}$, since the square of this term appears in front of the pseudoscalar field in the left-hand side of Equation (14). This effective mass depends on the value of the first invariant of the electromagnetic field $F_{ik} F^{ik}$. This finding is similar to the one known in the dilaton electrodynamics with the Lagrange term $\frac{1}{8}\Phi^2 F_{mn} F^{mn}$, where the scalar field Φ describes the dilaton. However, the fact that the coupling constant Ψ_0^{-2} enters the effective mass $M_{(\mathrm{eff})}$ allows us to speak about the axionically induced dilaton-like contribution of the electromagnetic field into the effective axion mass.

2.1.3. Master Equations for the Gravitational Field

The variation of the action functional (5) with respect to the metric gives the gravity field equations

$$R_{ik} - \frac{1}{2} R g_{ik} = \Lambda g_{ik} + \kappa T_{ik}^{(\mathrm{EMA})} + \kappa T_{ik}^{(\mathrm{A})}. \tag{16}$$

Here, the term

$$T_{ik}^{(\mathrm{A})} = \Psi_0^2\left[\nabla_i \phi \nabla_k \phi + \frac{1}{2} g_{ik}\left(V(\phi) - \nabla_p \phi \nabla^p \phi\right)\right] \tag{17}$$

is the stress–energy tensor of the pseudoscalar (axion) field, and the tensor

$$T_{ik}^{(\mathrm{EMA})} = \mathcal{L}'(\mathcal{I}) \cos\phi\left[\frac{1}{4} g_{ik} F_{mn} F^{mn} - F_{im} F_k^{\ m}\right] + g_{ik}\left[\mathcal{L}(\mathcal{I}) - \mathcal{I} \cdot \mathcal{L}'(\mathcal{I})\right] \tag{18}$$

contains all the contributions of the electromagnetic field. It coincides with the standard stress–energy tensor of the electromagnetic field, when $\phi = 0$ and $\mathcal{L}(\mathcal{I}) = \mathcal{I}$. The trace of the tensor (18)

$$T_{ik}^{(\mathrm{EMA})} g^{ik} = 4\left[\mathcal{L}(\mathcal{I}) - \mathcal{I} \cdot \mathcal{L}'(\mathcal{I})\right] \tag{19}$$

is generally nonvanishing; it is equal to zero only in the linear version of the theory. The total stress–energy tensor satisfies the condition

$$\nabla^k\left[T_{ik}^{(\mathrm{A})} + T_{ik}^{(\mathrm{EMA})}\right] = 0 \tag{20}$$

as the differential consequence of (6), (7), and (10).

3. Magnetized Universe: Bianchi-I Model

We apply the established theory to the anisotropic homogeneous cosmological model with magnetic field; the appropriate spacetime platform for this model is the Bianchi-I model (see, e.g., [10–16] and the references therein). The metric

$$ds^2 = dt^2 - a^2(t)dx^2 - b^2(t)dy^2 - c^2(t)dz^2 \tag{21}$$

depends on the cosmological time only. We assume that all physical quantities inherit this symmetry and also are a function of t only.

3.1. Exact Solution to the Electromagnetic Field Equations

With the fixed symmetry ansatz, Equation (7) standardly gives the solution for the magnetic field

$$F_{12} = const \equiv B_0\,, \tag{22}$$

and hint that the electric field parallel to the magnetic field $E(t) \equiv c(t)F^{30}$ appears as the result of the axion–photon coupling. Indeed, four equations (6) reduce to the following one:

$$\frac{d}{dt}\left\{\mathcal{L}'(\mathcal{I})[ab\cos\phi E - B_0\sin\phi]\right\} = 0\,, \tag{23}$$

and its solution is

$$E(t) = \frac{B_0}{ab}\tan\phi + \frac{\text{const}}{ab\cos\phi\ \mathcal{L}'(\mathcal{I})}\,. \tag{24}$$

For the sake of simplicity we consider the model, in which the electric field is equal to zero at the moment t_0; moreover, we assume that the initial value of the axion field is equal to πm ($m = 0, 1, \dots$), thus providing that the integration constant is equal to zero

$$E(t_0) = 0\,, \quad \phi(t_0) = \pi m \ \rightarrow\ \text{const} = 0\,. \tag{25}$$

With these initial conditions, we obtain the elegant formulas, first, for the electric field

$$E(t) = \frac{B_0}{ab}\tan\phi\,, \tag{26}$$

second, for the invariants of the electromagnetic field

$$F^*_{pq}F^{pq} = \frac{4B_0^2}{a^2b^2}\tan\phi\,, \quad F_{pq}F^{pq} = \frac{2B_0^2}{a^2b^2}\left[1 - \tan^2\phi\right], \tag{27}$$

third, for the invariant $\mathcal{I}$

$$\mathcal{I} = \frac{B_0^2}{2a^2b^2\cos\phi}\,. \tag{28}$$

3.2. Reduced Equation for the Axion Field

Equations (10) with (11) can be now transformed into

$$\ddot{\phi} + \frac{(abc)^{\cdot}}{abc}\dot{\phi} + m_A^2\sin\phi = -\frac{B_0^2\mathcal{L}'(\mathcal{I})\sin\phi}{2\Psi_0^2a^2b^2\cos^2\phi}\,, \tag{29}$$

where the dot denotes the derivative with respect to the cosmological time. There is also the following convenient form of this equation

$$\ddot{\phi} + \frac{(abc)^{\cdot}}{abc}\dot{\phi} = -\sin\phi\left[m_A^2 + \frac{\mathcal{I}\mathcal{L}'(\mathcal{I})}{\Psi_0^2\cos\phi}\right], \tag{30}$$

which shows explicitly that the formula $\phi = \pi n$ with integer n gives the series of exact solutions to the axion field equation in the case of the arbitrary nonlinear term $\mathcal{L}(\mathcal{I})$ with a finite derivative.

3.3. Reduced Equations for the Gravity Field

Equations (16) with (17) and (18) convert into four nonlinear differential equations of the second order

$$\left[\frac{\dot{a}}{a}\frac{\dot{b}}{b}+\frac{\dot{a}}{a}\frac{\dot{c}}{c}+\frac{\dot{b}}{b}\frac{\dot{c}}{c}\right] = \Lambda+\frac{1}{2}\kappa\Psi_0^2\left(V(\phi)+\dot{\phi}^2\right)+\kappa\mathcal{L}(\mathcal{I})\,, \tag{31}$$

$$\left[\frac{\ddot{b}}{b}+\frac{\ddot{c}}{c}+\frac{\dot{b}}{b}\frac{\dot{c}}{c}\right] = \Lambda+\frac{1}{2}\kappa\Psi_0^2\left(V(\phi)-\dot{\phi}^2\right)+\kappa\left[\mathcal{L}(\mathcal{I})-2\mathcal{I}\mathcal{L}'(\mathcal{I})\right], \tag{32}$$

$$\left[\frac{\ddot{a}}{a}+\frac{\ddot{c}}{c}+\frac{\dot{a}}{a}\frac{\dot{c}}{c}\right] = \Lambda+\frac{1}{2}\kappa\Psi_0^2\left(V(\phi)-\dot{\phi}^2\right)+\kappa\left[\mathcal{L}(\mathcal{I})-2\mathcal{I}\mathcal{L}'(\mathcal{I})\right], \tag{33}$$

$$\left[\frac{\ddot{b}}{b}+\frac{\ddot{a}}{a}+\frac{\dot{b}}{b}\frac{\dot{a}}{a}\right] = \Lambda+\frac{1}{2}\kappa\Psi_0^2\left(V(\phi)-\dot{\phi}^2\right)+\kappa\mathcal{L}(\mathcal{I})\,. \tag{34}$$

Since only the magnetic and electric fields directed along the axis $0z$ are the sources of the spacetime anisotropy, we can consider the truncated model with the so-called local isotropy, when $a(t) = b(t)$. In addition, we introduce the function $H = \frac{\dot{a}}{a}$ and can rewrite the independent gravity field equations as the following set:

$$H^2+2H\frac{\dot{c}}{c} = \Lambda+\frac{1}{2}\kappa\Psi_0^2\left(V(\phi)+\dot{\phi}^2\right)+\kappa\mathcal{L}(\mathcal{I})\,, \tag{35}$$

$$\left[\frac{\ddot{a}}{a}+\frac{\ddot{c}}{c}+\frac{\dot{a}}{a}\frac{\dot{c}}{c}\right] = \Lambda+\frac{1}{2}\kappa\Psi_0^2\left(V(\phi)-\dot{\phi}^2\right)+\kappa\left[\mathcal{L}(\mathcal{I})-2\mathcal{I}\mathcal{L}'(\mathcal{I})\right], \tag{36}$$

$$2\dot{H}+3H^2 = \Lambda+\frac{1}{2}\kappa\Psi_0^2\left(V(\phi)-\dot{\phi}^2\right)+\kappa\mathcal{L}(\mathcal{I})\,. \tag{37}$$

As usual, we see that Equation (36) is the differential consequence of (35) and (37).

3.4. Key Equations of the Model

The difference of Equations (35) and (37) yields

$$H\frac{\dot{c}}{c}-\dot{H}-H^2 = \frac{1}{2}\kappa\Psi_0^2\dot{\phi}^2\,, \tag{38}$$

and we immediately obtain the scale factor $c(t)$ in quadratures

$$c(t) = c(t_0)\frac{a(t)H(t)}{a(t_0)H(t_0)}\exp\left\{\frac{1}{2}\kappa\Psi_0^2\int_{t_0}^{t}\frac{dt}{H(t)}\dot{\phi}^2\right\}. \tag{39}$$

For the model with the local isotropy, it is convenient to use the new variable x introduced as follows:

$$x = \frac{a(t)}{a(t_0)}\,,\quad \frac{d}{dt} = xH\frac{d}{dx}\,. \tag{40}$$

In these terms, the scale factor (39) takes the form

$$c(x) = c(1)\,x\frac{H(x)}{H(1)}\exp\left[\frac{1}{2}\kappa\Psi_0^2\int_1^x z dz\phi'^2(z)\right], \tag{41}$$

and we obtain the pair of the *key equations* for two unknown functions $H(x)$ and $\phi(x)$:

$$\frac{1}{x^2}\,\frac{d}{dx}(x^3H^2) = \Lambda+\frac{1}{2}\kappa\Psi_0^2\left[2m_A^2(1-\cos\phi)-x^2H^2\phi'^2\right]+\kappa\mathcal{L}(\mathcal{I})\,. \tag{42}$$

$$\frac{1}{x^2}\frac{d}{dx}(x^4H^2\phi') + \frac{1}{2}\kappa\Psi_0^2x^3H^2\phi'^3 = -\sin\phi\left[m_A^2 + \frac{\mathcal{I}\mathcal{L}'(\mathcal{I})}{\Psi_0^2\cos\phi}\right]. \tag{43}$$

Here and below depending on the context, we use two equivalent forms for the metric coefficient $c(1) \equiv c(x=1) = c(t_0)$ and for the Hubble function $H(1) \equiv H(x=1) = H(t_0)$. We have to keep in mind now that the argument $\mathcal{I}$ of the nonlinear Lagrangian can be written as

$$\mathcal{I} = \frac{\omega^2}{x^4\cos\phi}, \quad \omega^2 \equiv \frac{B_0^2}{2a^4(t_0)}, \tag{44}$$

and that the scale factor $a(t)$ can be reconstructed using the formula

$$t - t_0 = \int_1^{\frac{a(t)}{a(t_0)}} \frac{dx}{xH(x)}. \tag{45}$$

4. Analysis of the Model: Exact Solutions and Numerical Study

The plan for the investigations of the presented model is the following: First of all, we consider the model with $\mathcal{L}(\mathcal{I}) = \mathcal{I}$, as an intermediate case, i.e., the axion field is presented in the nonlinear context, but the electrodynamics is linear. The main question which we have to discuss here can be formulated as follows: are the solutions for the electric field finite or infinite, or equivalently, is the model stable or unstable? The second step is to consider three particular nonlinear models, for which the Hubble functions are found analytically, but the axion field and electric field are obtained using numerical calculations.

4.1. Quasilinear Model

4.1.1. The Test of Instability

For the model with $\mathcal{L}(\mathcal{I}) = \mathcal{I}$, two key Equations (42) and (43) can be rewritten in the form:

$$\frac{1}{x^2}\frac{d}{dx}(x^3Y^2) = \Lambda^* + \kappa\Psi_0^2\left[\mu_A^2(1-\cos\phi) - \frac{1}{2}x^2Y^2\phi'^2 + \frac{1}{x^4\cos\phi}\right]. \tag{46}$$

$$\frac{1}{x^2}\frac{d}{dx}(x^4Y^2\phi') + \frac{1}{2}\kappa\Psi_0^2x^3Y^2\phi'^3 = -\sin\phi\left[\mu_A^2 + \frac{1}{x^4\cos^2\phi}\right]. \tag{47}$$

In order to simplify the numerical simulation, we introduced here the auxiliary quantities $Y(x)$, μ_A, Λ^* given by

$$H(x) = Y(x)H^*, \quad m_A = \mu_A H^*, \quad \Lambda = \Lambda^* H^{*2}, \quad H^* \equiv \frac{|B_0|}{\sqrt{2}a^2(t_0)\Psi_0}. \tag{48}$$

Similarly, we can introduce the dimensionless electric field $e(x)$ as follows:

$$E(x) = e(x)E^*, \quad E^* \equiv \frac{|B_0|}{a^2(t_0)} \quad \rightarrow \quad e(x) = \frac{\tan\phi(x)}{x^2}. \tag{49}$$

When $\phi \to \frac{\pi}{2}$, the electric field (26), the invariants of the electromagnetic fields (27), and the basic invariant (28) tend toward infinity. Respectively, the right-hand sides of the key Equations (46) and (47) also tend toward infinity in this limit. We have to test, whether the axion field ϕ can reach the catastrophic value $\phi = \frac{\pi}{2}$. For this purpose, we consider two submodels. In the first one, the initial value of the axion field is chosen as $\phi(t_0) = 0$; this value corresponds to the first minimum of the axion potential (11). In the second submodel, we assume that the axion field evolution starts with the value $\phi = \pi$, which relates to the first maximum of the axion potential.

4.1.2. The First Submodel Is Stable

When $\dot{\phi}(t_0) = 0$, we see that $\phi(x) \equiv 0$ is the exact solution to Equation (47). As for Equation (46), it can be directly integrated yielding

$$Y^2(x) = \frac{1}{x^3}Y^2(1) + \frac{1}{3}\Lambda^*\left(1 - \frac{1}{x^3}\right) + \kappa\Psi_0^2\left(\frac{1}{x^3} - \frac{1}{x^4}\right). \tag{50}$$

Since $E(x) = 0$ for this solution, we recover the well-known solution attributed to the Bianchi-I model with the pure magnetic field. Asymptotically, this solution describes the de Sitter model with $H \to \sqrt{\frac{\Lambda}{3}}$ and is characterized by isotropization $\frac{c}{a} \to const$.

When $\dot{\phi}(t_0) \neq 0$, the numerical analysis of the key Equations (46) and (47) shows that all the curves $\phi(x)$ are located below the horizontal line $\phi = \frac{\pi}{2}$. This means that the electric field E, Hubble function H and scale factors a, c take finite values, i.e., the catastrophic regime cannot be realized. We illustrate this fact using Figures 1–3.

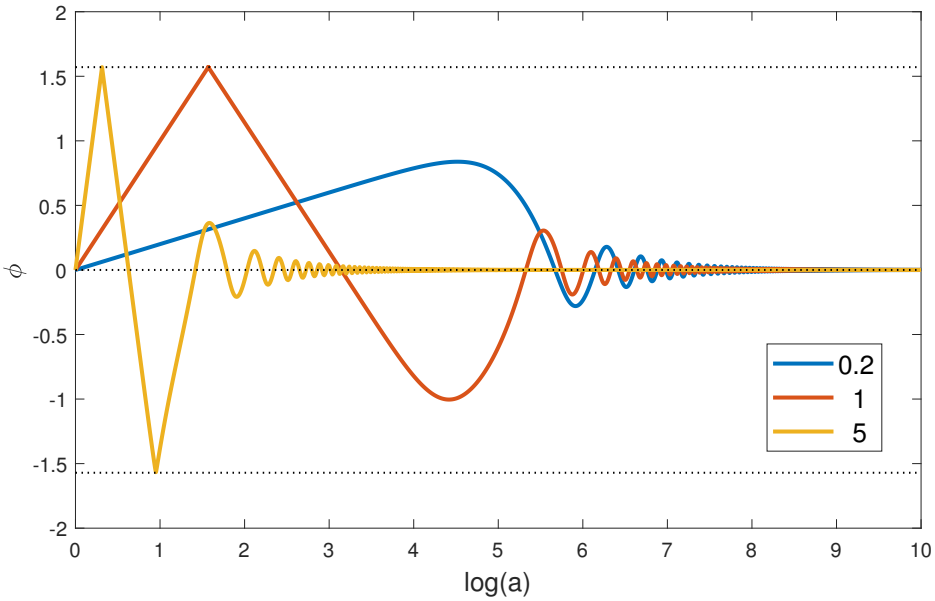

Figure 1. This figure illustrates the behavior of the axion field with the initial value $\phi(t_0) = 0$ as a function of the initial value of the axion field derivative $\dot{\phi}(t_0)$; three values of this parameter are fixed in the lower-right corner of the panel. All the values of the axion field ϕ belong to the interval $-\frac{\pi}{2} < \phi < \frac{\pi}{2}$. The character of evolution of the axion field can be characterized as damping oscillations. The sharpness of the first line in the zones of the first maximum and first minimum is the result of the choice of a special unified scale, which allowed us to visualize the oscillation pattern simultaneously for both: small and large values of the scale factor a.

For the model under discussion, the oscillatory regime of the axion field evolution is predetermined by the structure of Equation (47). Indeed, in the vicinities of the extrema points, when $\phi' \to 0$, the mentioned equation can be rewritten as

$$\phi'' = -\frac{1}{x^2Y^2}\left(\mu_A^2 + \frac{1}{x^4\cos^2\phi}\right)\sin\phi\,. \tag{51}$$

Clearly, the sign of the second derivative depends on the sign of the function $\sin\phi$: when $\phi > 0$, we see that $\phi'' < 0$, and we observe the maxima; when $\phi < 0$, we deal with the minima. If $\phi \to \frac{\pi}{2}$, the corresponding second derivative becomes large due to the term proportional to $\frac{1}{\cos^2\phi}$, this means that the degree of convexity/concavity of the graph increases, but the typical structure of the extrema is preserved. The damping of these

oscillations is provided by the multipliers of the type $\frac{1}{x^4}$ and $\frac{1}{x^2}$, which decrease when the reduced scale factor $x = \frac{a(t)}{a(t_0)}$ grows.

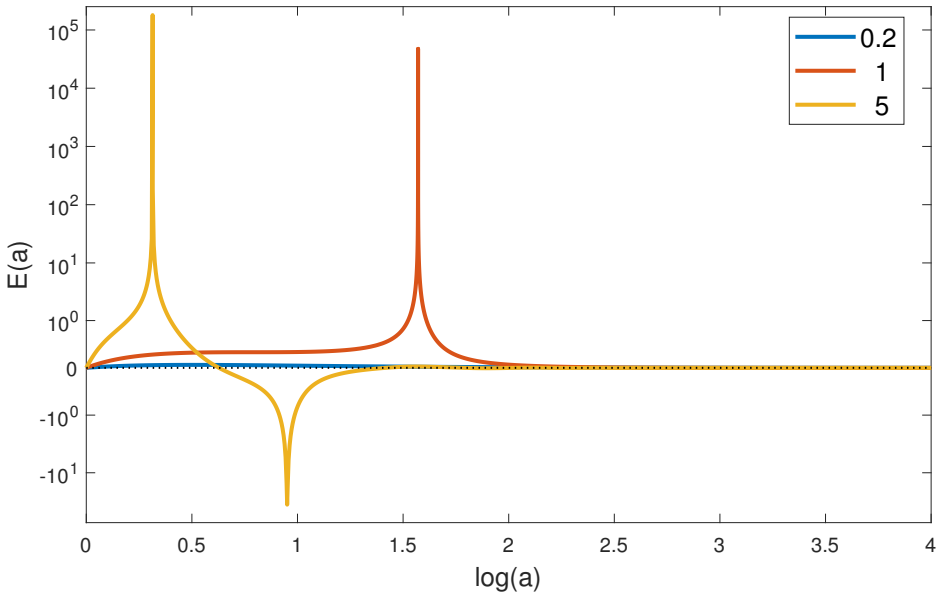

Figure 2. This figure presents three graphs of the reduced electric field $e(x) = \frac{E(x)}{E^*}$, which relate to the graphs of ϕ depicted on Figure 1. ($E^* = \frac{|B_0|}{a^2(t_0)}$). The electric field reaches very big values for the time moments, when the values of the axion field are close to $\pm\frac{\pi}{2}$. The behavior of the electric field inherits the oscillatory regime of the axion field; however, this property is hidden on the graph because of the incommensurability of the amplitudes of the first and second maxima of the corresponding graphs.

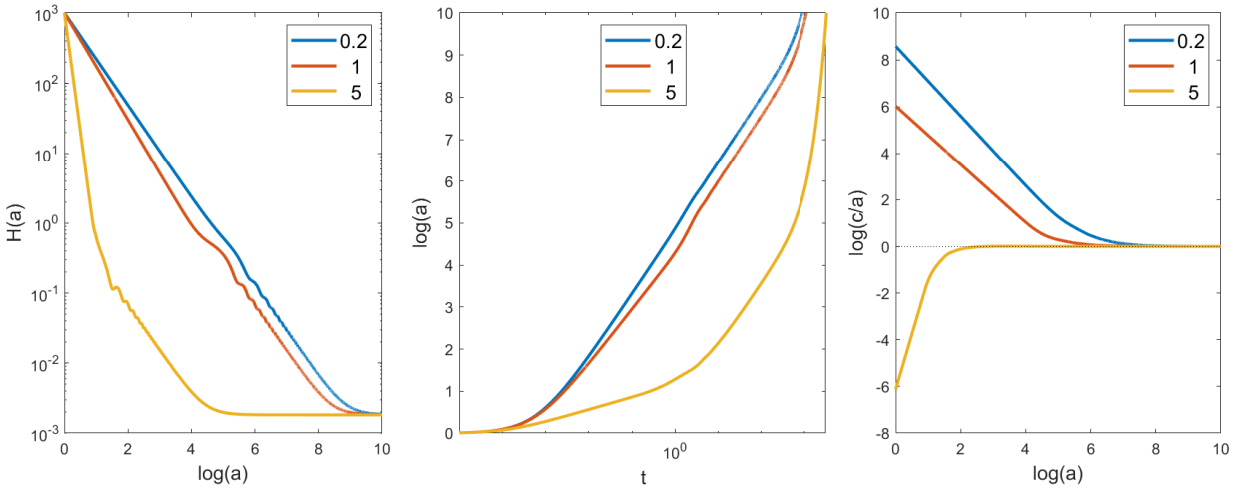

Figure 3. Illustrations of the geometric properties of the model. The behavior of the reduced Hubble function $Y(x) = \frac{H(x)}{H^*}$ is presented on the left panel; the central panel contains the graph of the scale factor $a(t)$; and the right panel presents the evolution of the ratio $\frac{c(t)}{a(t)}$. Oscillations of the axion field declare themselves in the form of ripples on the graph of the Hubble function. Asymptotically, $H(x)$ tends toward the de Sitter constant $\sqrt{\frac{\Lambda}{3}}$, and the ratio $\frac{c(t)}{a(t)}$ tends toward one, thus confirming the fact of the Universe isotropization.

4.1.3. The Second Submodel Is Unstable

When we put $\phi(t_0) = \pi$ and $\dot{\phi}(t_0) = 0$, we again obtain the constant exact solution $\phi \equiv \pi$ to Equation (47). The Hubble function is now described by the formula

$$Y^2(x) = \frac{1}{x^3}Y^2(1) + \frac{1}{3}\tilde{\Lambda}\left(1 - \frac{1}{x^3}\right) - \kappa\Psi_0^2\left(\frac{1}{x^3} - \frac{1}{x^4}\right), \tag{52}$$

where the redefined cosmological constant is $\tilde{\Lambda} = \Lambda^* + 2\kappa\Psi_0^2\mu_A^2$. Again, at $x \to \infty$, we obtain the de Sitter type behavior of the model.

When $\dot{\phi}(t_0) \neq 0$, the numerical analysis of the key Equations (46) and (47) gives principally different results: the horizontal line $\phi{=}\frac{\pi}{2}$ happens to be crossed for the arbitrary nonvanishing initial value of the derivative $\dot{\phi}(t_0)$. This submodel is unstable. We illustrate this fact by Figure 4.

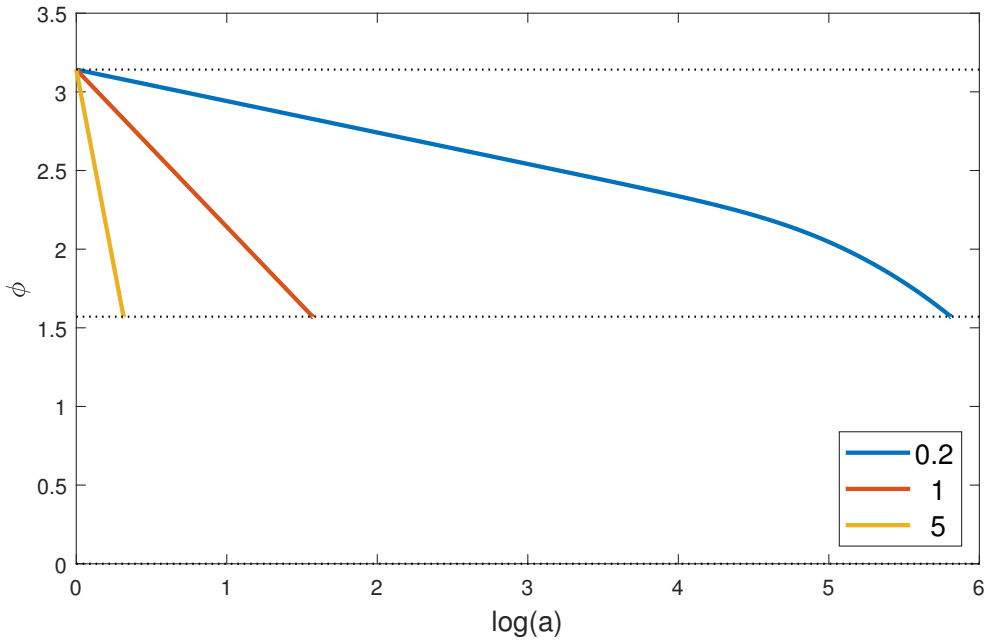

Figure 4. Illustrations of the behavior of the axion field with initial value $\phi(t_0){=}\pi$. The graphs are monotonic, and the axion field reaches the value $\phi = \frac{\pi}{2}$ for the finite value of the reduced scale factor x. The corresponding values of the electric field are infinite. The geometric characteristics of the Universe reveal singularity.

4.2. Analysis of the Behavior of Nonlinear Systems in the Vicinity of the First Minimum of the Axion Potential: Three Explicit Examples

4.2.1. Basic Equilibrium Solutions and Equation of Perturbation Dynamics

The first minimum of the axion potential corresponds to the value $\phi = 0$; we add to the axion field a small spatially homogeneous perturbation $\psi(t)$. In the leading order approximation, the electric field (26) vanishes, and the key Equation (42) takes the form

$$\frac{1}{x^2}\frac{d}{dx}(x^3H^2) = \Lambda + \kappa\mathcal{L}(\mathcal{I})\,. \tag{53}$$

Since now the invariant $\mathcal{I}$ is of the form $\mathcal{I} \to \frac{\omega^2}{x^4} \equiv z$, we can rewrite the key equation as follows:

$$-4z\frac{dH^2}{dz} + 3H^2 = \Lambda + \kappa\mathcal{L}(z)\,. \tag{54}$$

The solution for $H(x)$ can be presented in quadratures

$$H^2(x) = H^2(1)x^{-3} + \frac{\Lambda}{3}(1 - x^{-3}) - \frac{1}{4}\kappa\omega^{\frac{3}{2}}x^{-3}\int_{\omega^2}^{\omega^2 x^{-4}} d\xi\, \xi^{-\frac{7}{4}}\mathcal{L}(\xi)\,. \tag{55}$$

The scale factor $c(x)$ also can be simplified:

$$c(x) = c(1)\, x\frac{H(x)}{H(1)}\,. \tag{56}$$

In the first-order approximation with respect to $\psi(t)$, we obtain the equation

$$\frac{1}{x^2}\frac{d}{dx}\left[x^4H^2(x)\frac{d}{dx}\psi\right] + \psi\left[m_A^2 + \frac{\omega^2\mathcal{L}'(z)}{x^4\Psi_0^2}\right] = 0\,. \tag{57}$$

In the linear approximation, the electric field is proportional to ψ, i.e., $E(x) = \frac{\psi}{x^2}E^*$.

4.2.2. The First Example: Power-Law Lagrange Function

Integration in (55) with the function (8) gives

$$H^2(x) = H^2(1)x^{-3} + \frac{\Lambda}{3}(1 - x^{-3}) +$$

$$\kappa\left\{\frac{\omega^2}{x^4}(x-1) + \frac{\gamma}{(4\nu-3)}\left(\frac{\omega^2}{x^4}\right)^{\nu}\left(x^{4\nu-3} - 1\right)\right\}. \tag{58}$$

Asymptotically, we deal with the de Sitter law $H(x \to \infty) \to \sqrt{\frac{\Lambda}{3}}$.

Figure 5 illustrates the behavior of $H(x)$, of the scale factor $a(t)$ and of the ratio $\frac{c(t)}{a(t)}$ for this model. Figure 6 presents the corresponding graphs of the function $\psi(t)$.

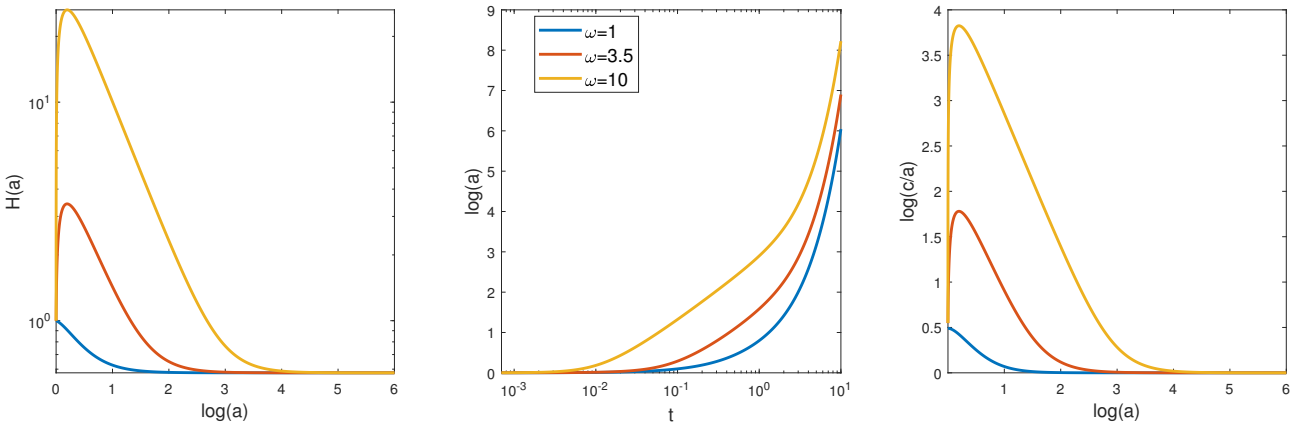

Figure 5. Illustration of the behavior of the Hubble function $H(x)$, of the scale factor $a(t)$ and of the ratio $\frac{c(t)}{a(t)}$ for a few values of the parameters ν and ω attributed to the Power-Law Lagrange function.

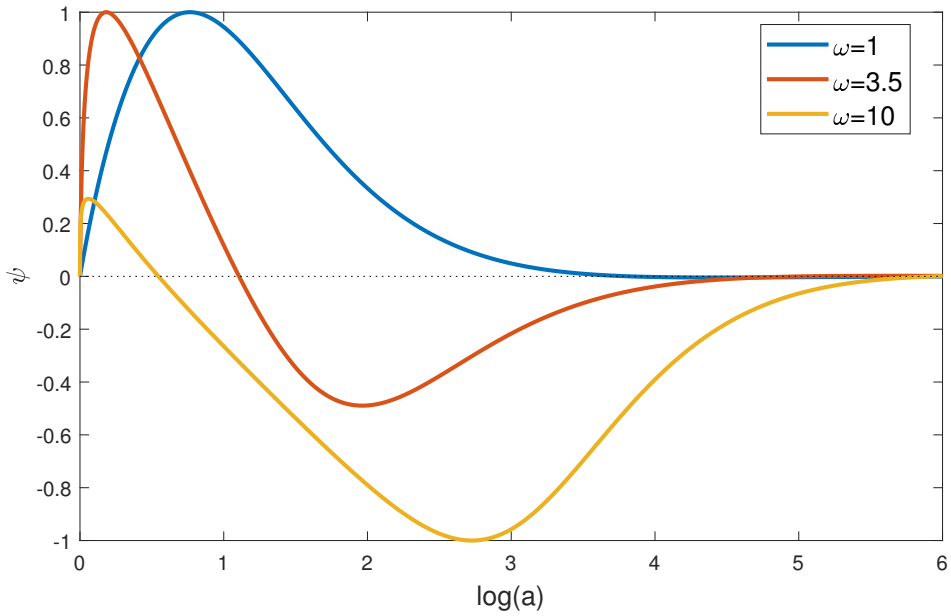

Figure 6. Illustration of the behavior of the function ψ for the model with Power-Law Lagrange function. Perturbations remain finite, and the model is stable.

4.2.3. The Second Example: Kohlrausch Type Function with $\gamma = \frac{1}{8}$

Now, we consider the Lagrange function (9) with $\gamma=\frac{1}{8}$. The function $H(x)$ can be presented in the explicit analytic form

$$H^2(x) = H^2(1)x^{-3} + \frac{\Lambda}{3}(1-x^{-3}) + 2\kappa\frac{\omega^3}{x^6}\left\{\omega^{\frac{1}{4}}\left(\frac{1}{\sqrt{x}}-1\right)+\exp\left(\omega^{\frac{1}{4}}\right)-\exp\left[\left(\frac{\omega}{x^2}\right)^{\frac{1}{4}}\right]\right\}. \quad (59)$$

Again, we deal with the asymptotically de Sitter type behavior; however, in contrast to the results for the quasilinear model, one can see that $H(x)$ and $\frac{c(t)}{a(t)}$ are nonmonotonic.

Figure 7 illustrates the behavior of $H(x)$, of the scale factor $a(t)$ and of the ratio $\frac{c(t)}{a(t)}$ for this model. Figure 8 presents the corresponding graphs of the function $\psi(t)$.

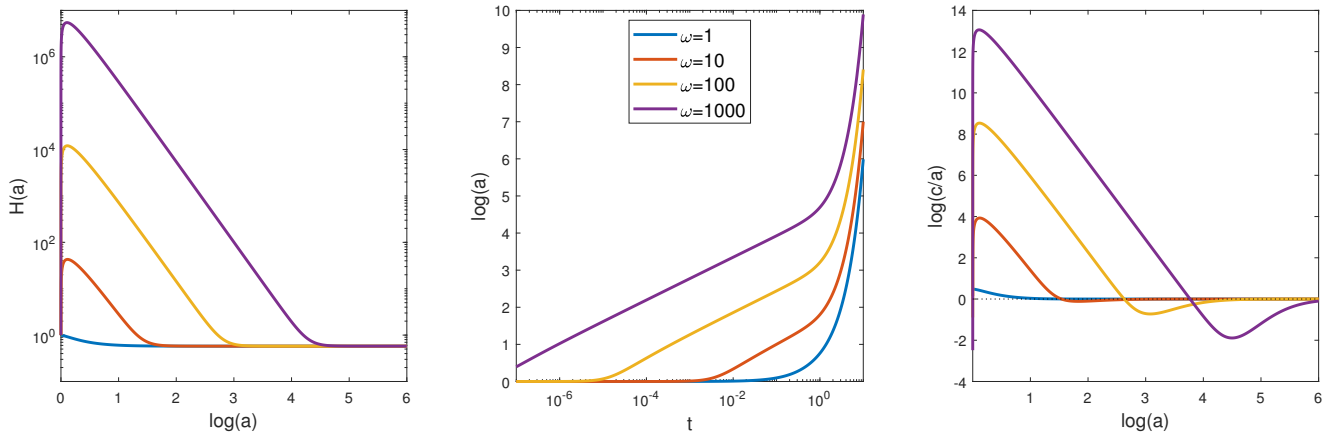

Figure 7. Illustration of the behavior of the function $H(x)$, $a(t)$ and of the ratio $\frac{c(t)}{a(t)}$ for the Kohlrausch model with $\gamma = \frac{1}{8}$.

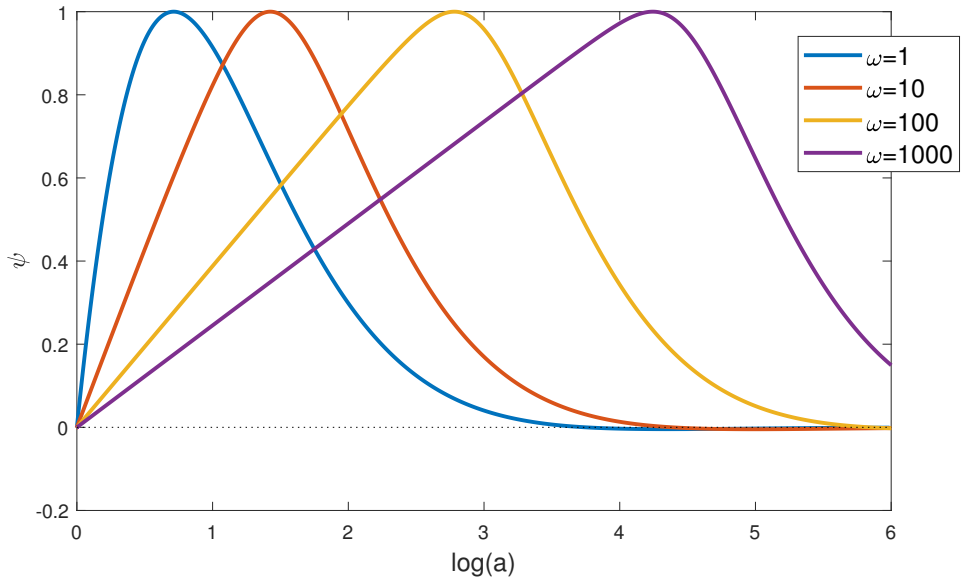

Figure 8. Illustration of the behavior of the function ψ for the Kohlrausch model with $\gamma = \frac{1}{8}$. Perturbations of the axion field remain finite and their moduli do not exceed the value $\frac{\pi}{2}$.

4.2.4. The Third Example: Kohlrausch Type Function with $\gamma = 2$ (Anti-Gaussian Function)

When we consider the model Lagrangian of the form

$$\mathcal{L}(\mathcal{I}) = \mathcal{I} + \beta \mathcal{I}^{\frac{11}{4}} \left[e^{\mathcal{I}^2} - 1 \right], \tag{60}$$

we obtain explicit analytic formula for the Hubble function; its square is

$$H^2(x) = H^2(1)x^{-3} + \frac{\Lambda}{3}(1 - x^{-3}) +$$

$$\kappa \left\{ \frac{\omega^2}{x^4}(x-1) + \frac{\beta}{8} \left[\left(\frac{\omega^2}{x^4} \right)^{\frac{11}{4}} (1 - x^8) + \left(\frac{\omega^2}{x^4} \right)^{\frac{3}{4}} \left(e^{\omega^4} - e^{\frac{\omega^4}{x^8}} \right) \right] \right\}. \tag{61}$$

Figure 9 illustrates the behavior of $H(x)$, of the scale factor $a(t)$ and of the ratio $\frac{c(t)}{a(t)}$ for this model. Figure 10 presents the corresponding graphs of the function $\psi(t)$.

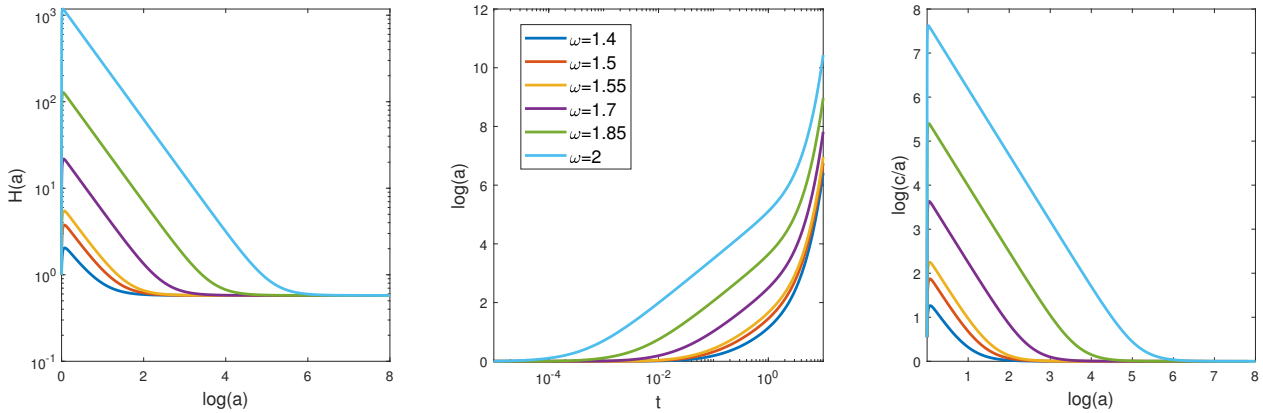

Figure 9. Illustration of the behavior of the functions $H(x)$, $a(t)$, and $\frac{c(t)}{a(t)}$ for the anti-Gaussian Lagrange function (60).

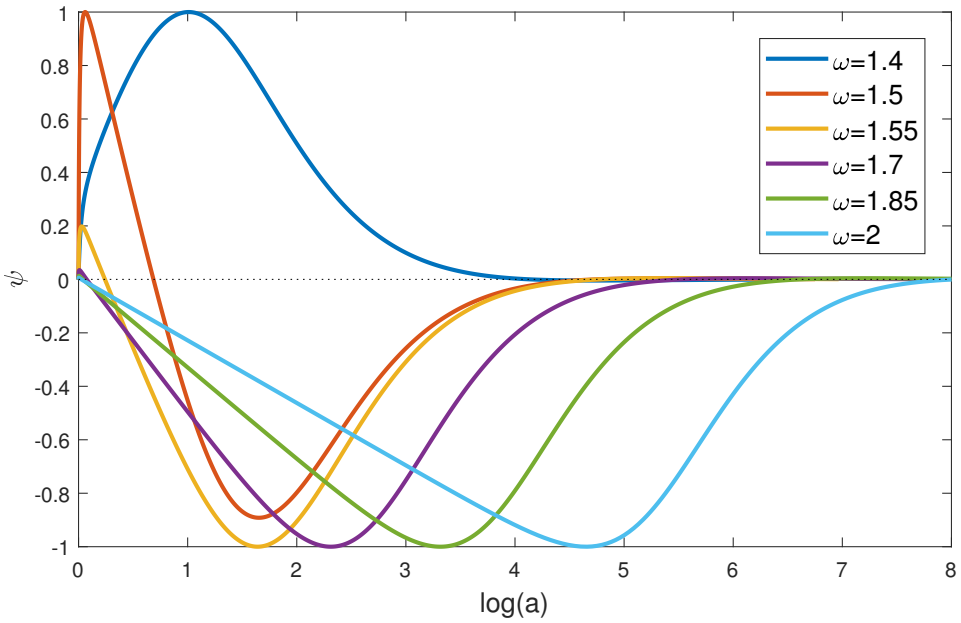

Figure 10. Illustration of the behavior of the function $\psi(t)$ for the anti-Gaussian Lagrange function (60).

5. Discussion and Conclusions

5.1. Axionically Induced Electric Field: Anomalies and Electric Flares

The mechanism of generation of the axionically induced electric field in the presence of the magnetic field is well known and well documented. This mechanism is based on the phenomenon of axion-photon coupling, and it has a lot of interesting applications (see, e.g., [5,6,17]). The new trend in the axion electrodynamics is connected with the elaboration of the nonlinear axion electrodynamics, which could have astrophysical and cosmological applications. In this sense, the early Universe with strong magnetic field [18–20], filled with the axionic dark matter [21–24], seems to be one of the most interesting objects of research. Indeed, it is well known that the dark matter axions interacting with the cosmic magnetic field produce the electric field; however, as the linear axion electrodynamics predicts, the contribution of such an electric field into the energetic balance of the Universe seems to be negligible, since the coupling constant of the axion–photon interactions is rather small, $\frac{1}{\Psi_0} = g_{A\gamma\gamma} < 1.47 \times 10^{-10}$ GeV^{-1}. The situation changes principally when we work with nonlinear axion electrodynamics. As we have shown above, the electric field with zero initial value can grow proportionally to the function $\tan\phi$. This means that if the dimensionless function ϕ, describing the evolution of the axion field, tends to the value $\phi = \frac{\pi}{2}$, the axionically induced electric field grows abnormally. We have studied the special question: is the catastrophic value $\phi = \frac{\pi}{2}$ reachable? The answer is negative; however, the maximum value of the electric field can be very large and even huge, depending on the initial value of the derivative $\dot{\phi}(t_0)$. As was shown above, the anomalous behavior of the electric field can be indicated as flare, since this electric field rapidly decreases in amplitude; this phenomenon can occur only once in the early Universe. If the initial value of the axion field is equal to $\phi(t_0) = \pi$, i.e., if it corresponds to the first maximum of the axion field potential, the catastrophic value $\phi = \frac{\pi}{2}$ is achieved inevitably; this model happens to be singular.

What are the physical consequences of such electric flares? From our point of view, one can expect, first, the creation of the electron–positron pairs; second, the acceleration of charged particles; and third, the emission of the electromagnetic waves by these accelerated particles.

5.2. On the Electron–Positron Pair Creation in the Axionically Induced Electric Field

According to Schwinger's formula, the probability of the electron–positron pair creation in vacuum under the influence of a strong electric field E is estimated to be the following:

$$\mathcal{W} = \frac{e^2E^2}{4\pi^3\hbar^2}\exp\left(-\frac{E_{(crit)}}{E}\right), \quad E_{(crit)} = \frac{\pi m_e^2}{\hbar e}, \quad (c=1). \tag{62}$$

Clearly, the nonlinear axion electrodynamics of the early magnetized Universe does not prohibit the anomalous electric field energy to overcome the threshold $2m_ec^2$, thus providing the creation of the electron–positron pairs in vacuum.

5.3. Particle Acceleration

If the initial three-momenta of the electron and positron, born in the strong electric field, are equal to zero, these particles begin to move along the direction $0z$ indicated by the parallel electric and magnetic fields. For this field configuration, the particles have only two components of the velocity four-vector: U_z and $U_0 = \sqrt{1 + c^{-2}(t)U_z^2}$, and the longitudinal component of the acceleration four-vector. From the equation of the particle dynamics

$$\frac{dP_j}{ds} = \Gamma^k_{jl}P_k\frac{P^l}{m_e} + \frac{e}{m_e}F_{jl}P^l, \tag{63}$$

where $P_i = m_eU_i$ is the particle four-momentum, we obtain for the longitudinal acceleration and velocity, respectively, the following relationships:

$$\frac{dU_z}{dt} = -\frac{ec(t)B_0}{m_ea^2(t)}\tan\phi(t), \quad U_z(t) = -\frac{eB_0}{m_e}\int_{t_0}^{t}dt'\frac{c(t')}{a^2(t')}\tan\phi(t'). \tag{64}$$

These kinematic characteristics depend on time, and thus, we deal with the nonuniform accelerated motion. Clearly, electrons and positrons move in opposite directions and can take part in the process of anomalous acceleration, if $\phi(t) \to \frac{\pi}{2}$.

5.4. On the Radiation of Electromagnetic Waves by the Charged Particles Accelerated by the Axionically Induced Electric Field

The nonuniformly moving particles emit the electromagnetic wave. We consider the radiation of particles, which have the parallel three-velocity $\vec{v}$ and three-acceleration $\vec{w}$. In this case, the standard formulas for the radiation intensity per single solid angle has the form

$$\frac{dI}{d\Omega} = \frac{e^2}{4\pi}\frac{w^2\sin^2\theta}{(1-v\cos\theta)^6}, \quad v = |\vec{v}|, \quad w = |\vec{w}|, \quad (c=1), \tag{65}$$

where θ is the angle between the axis $0z$ and the direction to the observation point (see, e.g., [25]). In our case, for the very sharp peak of the electric flare, we can use the formulas $v \to \left|\frac{U_z}{U_0}\right|$ and $w \to \frac{dU_z}{dt}$ (see (64)). In the case of the anomalous axionically induced electric field, the charged particle born in this field can reach the ultrarelativistic state of motion, and the radiation is focused in the small angle θ. The intensity of radiation is proportional to $B_0^2\tan^2\phi$. In other words, one can expect that the directions $\theta = 0$ and $\theta = \pi$ are marked by the extra portions of light.

5.5. Conclusions

We presented the new version of the nonlinear extension of the Einstein–Maxwell-axion theory, and based on this theory, we can propose the following scenario of the evolution of the spatially homogeneous early magnetized Universe.

1. Let the axion field evolution start with zero value $\phi(t_0) = 0$ and with the nonvanishing derivative $\dot{\phi}(t_0) \neq 0$; in the presence of the cosmological magnetic field, the axion–photon coupling provides the creation of the axionically induced electric

field parallel to the magnetic field; in its turn, such electromagnetic field configuration produces a new portion of axions, thus unwinding the spiral of the nonlinear axion–photon interactions.

2. In the process of evolution, the axion field and its derivative remain finite; the axion field itself happens to be trapped in the zone $-\frac{\pi}{2} < \phi < \frac{\pi}{2}$ and thus does not play an essential role in the Universe expansion.
3. The axionically induced electric field, in contrast to the axion field, can reach anomalously large values, when $\phi \to \frac{\pi}{2}$; the so-called electric flares can appear, and the electromagnetic contribution to the sources of the gravity field can become essential.
4. The geometric characteristics of the Universe, such as scale factors and their derivatives, remain nonsingular at $t > t_0$ and inherit the oscillatory behavior of the electromagnetic sources; when the cosmological constant is nonvanishing, the final stage of the Universe evolution is of the de Sitter type and thus corresponds to the instruction about the late-time accelerated expansion.
5. The axionically induced anomalous electric field produces the electron–positron pairs and accelerates the born charged particles; the accelerated charged particles emit the electromagnetic waves, which are focused in the direction pointed by the parallel magnetic and electric fields; these flares can take part in the formation of fluctuations of the cosmic microwave background.

In the next work, we hope to revive this scenario by adding estimations and other necessary details.

Author Contributions: Conceptualization, A.B.B.; methodology, A.B.B. and V.V.B.; formal analysis, A.B.B. and V.V.B.; investigation, A.B.B., V.V.B., and A.F.N.; writing—original draft preparation, A.B.B.; writing—review and editing, A.B.B. and A.F.N.; visualization, V.V.B. All authors have read and agreed to the published version of the manuscript.

Funding: This research was funded by the Russian Foundation for Basic Research (Grant N 20-52-05009).

Institutional Review Board Statement: Not applicable.

Informed Consent Statement: Not applicable.

Data Availability Statement: The study did not report any data.

Acknowledgments: A.B. is grateful for the Russian Foundation for Basic Research for financial support (Grant N 20-52-05009). This paper was supported by the Kazan Federal University Strategic Academic Leadership Program.

Conflicts of Interest: The authors declare no conflict of interest.

References

1. Peccei, R.D.; Quinn, H.R. CP conservation in the presence of instantons. *Phys. Rev. Lett.* **1977**, *38*, 1440–1443. [CrossRef]
2. Weinberg, S. A new light boson? *Phys. Rev. Lett.* **1978**, *40*, 223–226. [CrossRef]
3. Wilczek, F. Problem of strong P and T invariance in the presence of instantons. *Phys. Rev. Lett.* **1978**, *40*, 279–282. [CrossRef]
4. Ni, W.-T. Equivalence principles and electromagnetism. *Phys. Rev. Lett.* **1977**, *38*, 301–304. [CrossRef]
5. Sikivie, P. Experimental tests of the "invisible" axion. *Phys. Rev. Lett.* **1983**, *51*, 1415–1417. [CrossRef]
6. Wilczek, F. Two applications of axion electrodynamics. *Phys. Rev. Lett.* **1987**, *58*, 1799–1802. [CrossRef] [PubMed]
7. Jackson, J.D. *Classical Electrodynamics*; John Wiley and Sons: New York, NY, USA, 1999.
8. Balakin, A.B.; Galimova, A.A. Towards nonlinear axion-dilaton electrodynamics: How can axionic dark matter mimic dilaton-photon interactions? *Phys. Rev. D* **2021**, *104*, 044059. [CrossRef]
9. Kohlrausch, R. Theorie des elektrischen Ruckstandes in der Leidner Flasche. *Ann. Phys. Chem.* **1854**, *91*, 56–82. [CrossRef]
10. Turner, M.S.; Widrow, L.M. Inflation-produced, large-scale magnetic fields. *Phys. Rev. D* **1988**, *37*, 2743–2769. [CrossRef]
11. Grasso, D.; Rubinstein, H.R. Magnetic fields in the early Universe. *Phys. Rept.* **2001**, *348*, 163–266. [CrossRef]
12. Lee, D.-S.; Lee, W.; Ng, K.-W. Primordial magnetic fields from dark energy. *Phys. Lett. B* **2002**, *542*, 1–7. [CrossRef]
13. Giovannini, M. The magnetized Universe. *Int. J. Mod. Phys. D* **2004**, *13*, 391–502. [CrossRef]
14. Bronnikov, K.A.; Chudaeva, E.N.; Shikin, G.N. Magneto-dilatonic Bianchi-I cosmology: Isotropization and singularity problems. *Class. Quantum Gravity* **2004**, *21*, 3389–3403. [CrossRef]

15. Bamba, K.; Odintsov, S.D. Inflation and late-time cosmic acceleration in non-minimal Maxwell-$F(R)$ gravity and the generation of large-scale magnetic fields. *J. Cosmol. Astropart. Phys.* **2008**, *4*, 24. [CrossRef]
16. Balakin, A.B. Magnetic relaxation in the Bianchi-I universe. *Class. Quantum Gravity* **2007**, *24*, 5221–5245. [CrossRef]
17. Balakin, A.B.; Muharlyamov, R.K.; Zayats, A.E. Axion-induced oscillations of cooperative electric field in a cosmic magneto-active plasma. *Eur. Phys. J. D* **2014**, *68*, 159. [CrossRef]
18. Novello, M.; Goulart, E.; Salim, J.M.; Perez Bergliaffa, S.E. Cosmological effects of nonlinear electrodynamics. *Class. Quantum Gravity* **2007**, *24*, 3021–3036. [CrossRef]
19. Kruglov, S.I. Universe acceleration and nonlinear electrodynamics. *Phys. Rev. D* **2015**, *92*, 123523. [CrossRef]
20. Övgün, A.; Leon, G.; Magaña, J.; Jusufi, K. Falsifying cosmological models based on a non-linear electrodynamics. *Eur. Phys. J. C* **2018**, *78*, 462. [CrossRef]
21. Duffy, L.D.; van Bibber, K. Axions as dark matter particles. *New J. Phys.* **2009**, *11*, 1050088. [CrossRef]
22. Steffen, F.D. Dark Matter candidates—Axions, neutralinos, gravitinos, and axinos. *Eur. Phys. J. C* **2009**, *59*, 557–588. [CrossRef]
23. Marsh, D.J.E. Axion Cosmology. *Phys. Rept.* **2016**, *643*, 1–79. [CrossRef]
24. Sikivie, P. Invisible axion search methods. *Rev. Mod. Phys.* **2021**, *93*, 15004. [CrossRef]
25. Landau, L.D.; Lifshitz, E.M. *The Classical Theory of Field*; Pergamon Press: Oxford, UK, 1971.